JOURNAL OF MATERIALS SCIENCE 29 (1994) 4399–4403

The role of ε-martensite in the impact toughness of an Fe–17Mn alloy

D. Q. WANG, H. F. LOPEZ
Materials Department, College of Engineering and Applied Science, University of Wisconsin – Milwaukee, PO Box 784, Milwaukee, WI 53201, USA

The influence of ε-martensite on the cryogenic toughness of an Fe–17 wt% Mn alloy was studied in this work. Alloys were tempered at various temperatures in order to systematically increase the volume fraction of ε-martensite. This was followed by Charpy impact testing conducted at room temperature and at −196 °C. The experimental results indicated that although room-temperature toughness was not influenced by the ε-martensite content, the cryogenic toughness was strongly dependent on the volume fraction of ε-martensite. In particular, with the exception of the alloys tempered at 400 and 450 °C, the impact toughness consistently increased with ε-martensite content. Microstructural and fractographic evaluations using SEM and TEM suggested that the toughness improvements were attributed to the $\varepsilon \rightarrow \alpha$ stress-induced martensite transformation. No microstructural evidence was found which could be ascribed to an effect of ε-martensite on the low-temperature embrittlement exhibited by Fe–Mn alloys tempered at 400–450 °C.

1. Introduction

The development of Fe–Mn alloys for potential applications in cryogenic environments has been an area of extensive research [1–8]. Among the advantages of these alloys is their remarkable strength and toughness at liquid nitrogen temperatures. These alloys also possess relatively low magnetic permeabilities, which make them attractive candidates for applications in high magnetic superconducting fields [2]. The cryogenic properties of Fe–Mn alloys are strongly influenced by alloying additions and by the phases present [3–6]. Manganese contents in excess of 8 wt % promote the formation of hexagonal ε-martensites [2–4], whereas Al additions effectively suppress the $\gamma \rightarrow \varepsilon$ transformation [7, 8].

The effect of ε-martensite on the cryogenic properties of Fe–Mn alloys is not well understood. Sato *et al.* [9] examined the plastic deformation of an Fe–30Mn single crystal which exhibits the $\gamma \rightarrow \varepsilon$ martensitic transformation. In their work they found that ε-martensite plates act as strong obstacles against dislocation motion, leading to large crystal hardening. Furthermore, strain-induced phase transformations such as $\gamma \rightarrow \alpha + \varepsilon$ or $\varepsilon \rightarrow \alpha$ have been accepted as causes of strengthening by work-hardening in Fe–Mn alloys [10–13]. Nevertheless, observations of low-temperature brittleness in Fe–Mn alloys have been attributed to the presence of ε-martensite [6, 14, 15] despite the lack of evidence to link the ε-phase with the low-temperature brittleness.

The nature of the low-temperature embrittlement exhibited by some Fe–Mn alloys is not clear. At low Mn contents (~ 5 wt %), Fe–Mn alloys seem to be sensitive to temper embrittlement, with the fracture mode being predominantly transgranular cleavage [6]. As the Mn content increases, the fracture mode changes to intergranular failure without detrimental effects on the alloy strength or toughness [1]. Other factors thought to be responsible for low-temperature embrittlement in Fe–Mn alloys include the segregation of impurities at grain boundaries [4].

Microstructurally, upon quenching from the austenite region, Fe–Mn alloys give rise to a mixture of $\alpha + \varepsilon + \gamma$ (for < 20 wt % Mn), $\gamma + \varepsilon$ (20 to 30 wt % Mn), or stable austenite for > 30 wt % Mn [2]. In all cases, low-temperature brittleness has been reported [2–4]. Furthermore, the lack of embrittlement observed in some high-Mn alloys (25–30 wt % Mn) has been attributed to the absence of significant amounts of ε-martensite [3]. In contrast, it has been found that the ductile–brittle transition temperature falls with increasing Mn content, while the alloys exhibit significant improvements in cryogenic strength [1].

As mentioned before, the effect of ε-martensite on the cryogenic properties of Fe–Mn alloys is not clearly understood, Hence the present work is aimed at investigating the effect of ε-martensite on the cryogenic impact toughness of an Fe–17 wt % Mn alloy.

2. Experimental procedure

The Fe–Mn alloys were cast after melting in an induction furnace under an inert atmosphere. Alloy slabs of composition Fe–16.4 wt % Mn, 0.05 wt % C, 0.22 wt % Si, 0.015 wt % P, 0.013 wt % S were cast and then forged into 14 mm × 14 mm slabs. This was followed by heating in a vacuum at 920 °C for 5 h and furnace-cooling. This treatment was used to eliminate the forging-induced texture.

0022–2461

Subsequently, the alloys were homogenized by austenitizing at 920 °C for 2 h, followed by water cooling and tempering for 1 h at temperatures between 300 and 750 °C. These treatments were chosen to minimize the effect of preferred orientations on the subsequent X-ray analyses. The transformation temperatures of the alloy were established from dilatometric studies. Furthermore, the relative volume fractions of phases present were determined by X-ray diffraction by direct comparisons of the integrated intensities of the $(2\,0\,0)_\gamma$, $(1\,0\,\bar{1}\,1)_\varepsilon$ and $(2\,0\,0)_\alpha$ peaks.

Following the heat treatment, ASTM Charpy impact specimens were tested at room temperature and at liquid nitrogen temperature (− 196 °C). Microstructural and fractographic evaluations were conducted using optical, scanning and transmission electron microscopy.

3. Results

3.1. Influence of tempering treatment

Optical microscopy indicated that the microstructure exhibited by the alloys subjected to various tempering treatments were basically similar. In all cases, intercrossing bands of ε-martensite were uniformly distributed in the matrix as shown in Fig. 1. TEM analyses of the phases present indicated that the martensitic bands were composed of large numbers of parallel ε-martensite plates (Fig. 2a and b). Furthermore, the presence of γ and α phases, as well as their relative plane orientations, was determined from electron diffraction patterns as shown in Fig. 3.

Measurements of lattice parameters for the ε, γ, and α phases gave $a_\varepsilon = 0.2532$ nm, $c_\varepsilon = 0.4083$ nm, $a_\gamma = 0.3581$ nm, and $a_\alpha = 0.2878$ nm, respectively. The relative volume fractions of the ε, γ, and α phases determined from X-ray diffraction measurements for the different tempering times are given in Table I. According to this table, as the tempering temperature is raised, the relative volume fraction of ε-martensite increases. The maximum content of ε-martensite occurred at 600 °C tempering, whereas the maximum amount of γ phase was found to exist at 450 °C tempering.

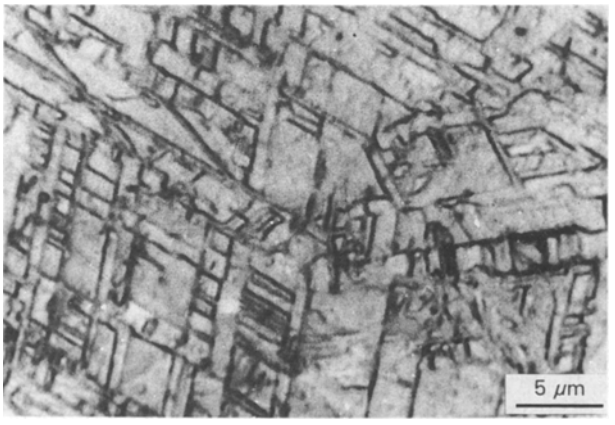

Figure 1 Optical metallography showing intercrossing ε-martensite bands.

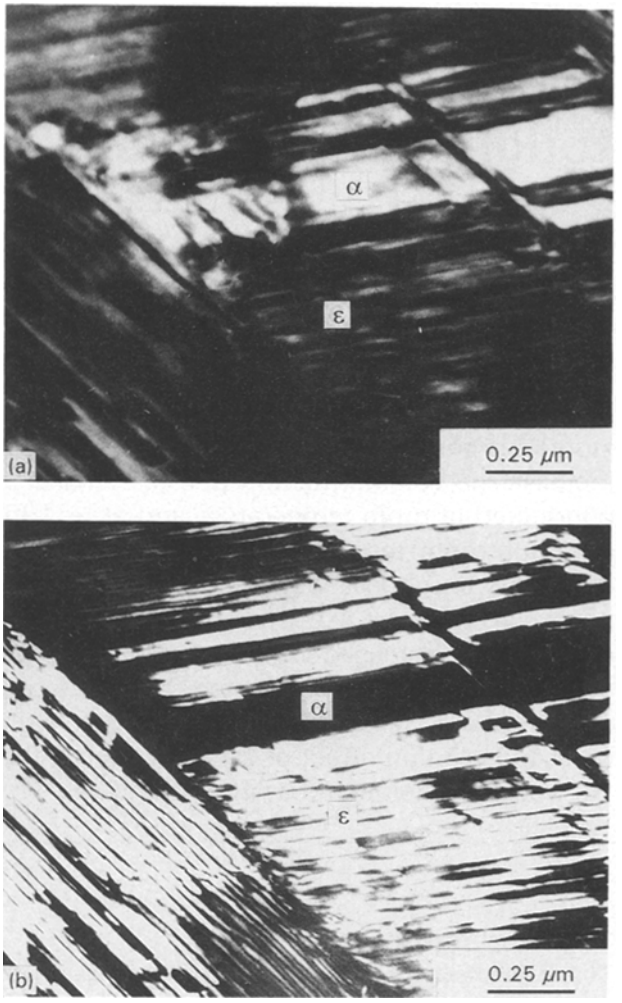

Figure 2 TEM micrographs showing twinned α- and ε-martensite plates: (a) bright-field, (b) dark-field image.

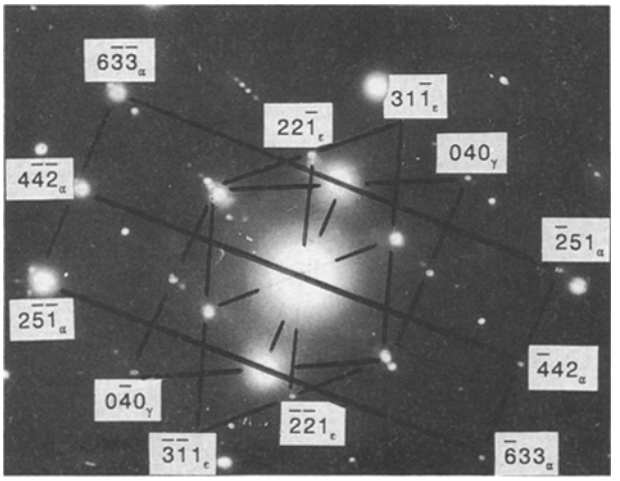

Figure 3 Electron diffraction patterns of γ, ε and α phases in Fe–17Mn alloy.

Dilatometric evaluations carried out at cooling and heating rates of 10 °C min^{-1} gave the following transformation points: $A_s = 545 \pm 5$ °C, $A_f = 565 \pm 5$ °C, $M_s = 302 \pm 5$ °C and $M_f = 285 \pm 5$ °C.

The influence of the tempering temperature on the size of newly precipitated grains produced within the prior austenite grains by the $\gamma \rightarrow \alpha + \varepsilon$ transformation is shown in Fig. 4. According to this figure, tempering

TABLE I Volume fractions of phases present in Fe–17Mn alloy

Sample no.	Treatment	Content (vol %)		
		f_ε	f_γ	f_α
1	300 °C 1 h, WQ[a]	68.1	17.0	14.9
2	350 °C 1 h, WQ	70.2	20.1	9.7
3	400 °C 1 h, WQ	69.8	20.7	9.5
4	450 °C 1 h, WQ	72.3	21.9	5.8
5	500 °C 1 h, WQ	75.0	21.0	4.0
6	550 °C 1 h, WQ	81.3	14.1	4.6
7	600 °C 1 h, WQ	84.0	12.3	3.7
8	650 °C 1 h, WQ	79.9	10.1	10.0
9	700 °C 1 h, WQ	71.4	13.5	15.1
10	750 °C 1 h, WQ	68.5	15.5	16.0

[a] Water quench.

below 600 °C does not have a significant influence on the resultant grain size. However, at temperatures beyond 600 °C, the grains containing the $\alpha + \varepsilon$ phases are no longer stable and the material reverts to austenite. Consequently, at 700 °C the grain size corresponds to that of prior austenite. This agrees with the dilatometric evaluations of this work, which indicate that the transformation to austenite should start at temperatures above 545 °C. (A_s).

3.2. Alloy toughness

Table II shows the alloy impact toughness at room temperature and at − 196 °C for the various tempering treatments. According to this table, room-temperature toughness is not significantly influenced by the tempering treatment. However, appreciable differences exist in the low-temperature toughness. Fig. 5 depicts the relationship between low-temperature toughness and ε-martensite content. From this figure it can be observed that there is a low-temperature embrittlement trough at 400–450 °C. Above this tempering range, the alloy impact toughness increases with the ε-martensite content. The maximum impact toughness is found to coincide with the maximum volume fraction of ε-martensite.

Finally, with the exception of the 400 and 450 °C temperings, the fracture surfaces of the specimens impacted at − 196 °C were ductile. Fig. 6 shows typical dimpled fracture appearances associated with ductile failures. Since in all cases ε-martensite was present, this suggests that the presence of the ε phase does not cause low-temperature brittleness.

TABLE II Impact toughness at room temperature − 196 °C in Fe–17 Mn alloy

Sample no.	Treatment	Impact toughness (kg m)	
		23 °C	− 196 °C
1	300 °C 1 h, WQ	11.83	4.30
2	350 °C 1 h, WQ	9.62	6.93
3	400 °C 1 h, WQ	10.10	2.94
4	450 °C 1 h, WQ	9.37	3.44
5	500 °C 1 h, WQ	10.28	7.52
6	550 °C 1 h, WQ	11.90	7.80
7	600 °C 1 h, WQ	10.94	8.40

4. Discussion

4.1. Low-T brittleness

It is generally accepted that Fe–Mn alloys can be susceptible to low-temperature brittleness, but the mechanistic aspects have not been investigated in detail. It has been suggested that ε-martensite promotes alloy brittleness at cryogenic temperatures [6, 14, 15] in contrast with the evidence found in this research. In the present work, the volume fraction of ε-martensite was systematically increased by appropriate tempering treatments. As a result, the effect of increasing volume fractions of ε-martensite on the cryogenic toughness was established.

The experimental outcome indicated that the alloy impact toughness at − 196 °C increases with the volume fraction of ε-phase (Fig. 5). Nevertheless, the cryogenic toughness drops for alloys tempered in the temperature range 400–450 °C. Although there was no noticeable embrittlement at room temperature, the embrittlement trough found at − 196 °C suggested that temper embrittlement occurred under these conditions. Apparently, impurity segregation during tempering at 400–450 °C was large enough to lock

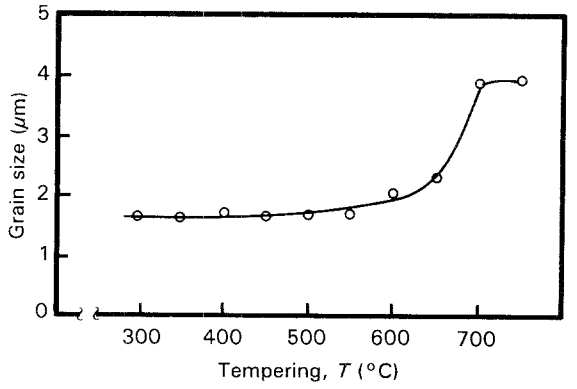

Figure 4 Influence of tempering temperature on the size of precipitated grains containing $\alpha + \varepsilon$ phases.

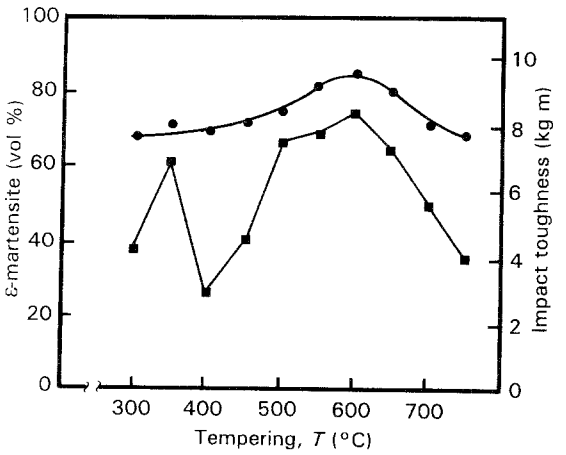

Figure 5 Relation between (■) impact toughness and (●) volume fraction of ε-martensite in Fe–17Mn alloy.

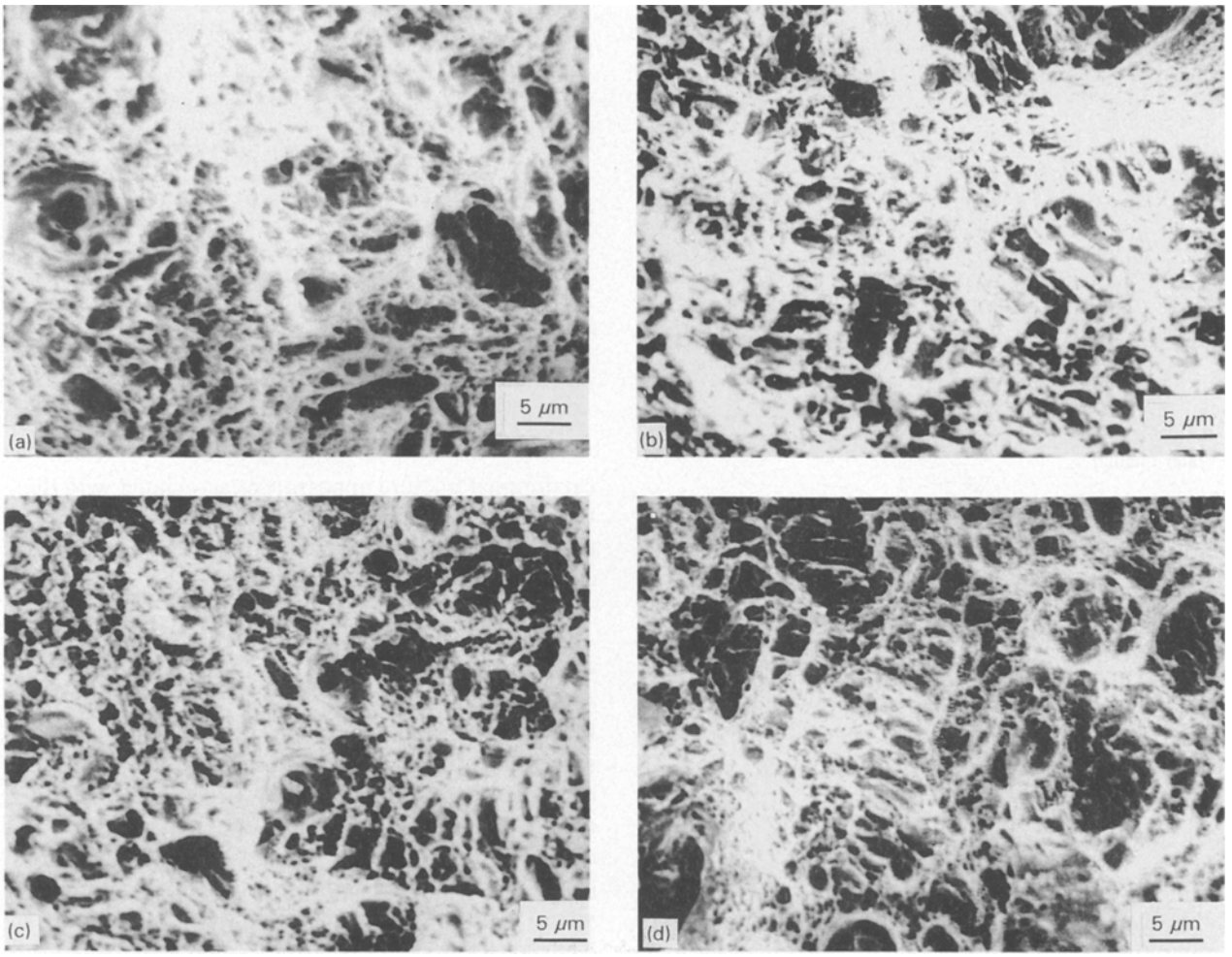

Figure 6 SEM fractographs showing low-temperature ductile dimpled fractures for various tempering temperatures in Fe–17Mn alloy: (a) 300 °C, (b) 500 °C, (c) 600 °C, (d) 700 °C.

dislocation motion and thus provide a "weak" fracture path. Since the volume fraction of ε-martensite consistently increased with tempering without raising the embrittling effect, this phase can be ruled out as the embrittling agent. This is further confirmed by the evidence of beneficial effects induced by ε-martensite on the cryogenic toughness of Fe–Mn alloys [16].

Although the low-temperature toughness of the Fe–17Mn alloy was inferior to that exhibited at room temperature, it improved considerably with increasing volume fractions of ε-martensite (Fig. 5). These observations were further supported by fractographic observations. In all cases (with the exception of 400–450 °C temperings) the fracture surfaces of the specimens impacted at − 196 °C corresponded to a transgranular ductile dimple fracture mode (see Fig. 6a–d).

Tempering at temperatures beyond 600 °C led to significant reductions in alloy toughness. According to the dilatometric measurements, at these temperatures austenite is the stable phase. Hence it was expected that the α- and ε-martensites would revert to the γ phase. Upon subsequent alloy cooling the $\gamma \rightarrow \alpha$ transformation was apparently favoured over the $\gamma \rightarrow \varepsilon$ transformation, thus reducing the volume fraction of ε phase. As a result, the alloys tempered at temperatures above 600 °C exhibited lower cryogenic toughnesses (Table II).

4.2. Low-*T* toughness

According to the literature [9], ε-martensite is mechanically unstable. Hence, during plastic deformation, this phase transforms into α-martensite. Consequently, the stress-induced phase transformation is thought to account for the increases in alloy strength and toughness at cryogenic temperatures [10–13]. Furthermore, it has been found [9] that ε plates are extremely resistant to the motion of dislocations crossing them. Thus, the presence of ε plates is essential in producing large hardening against dislocation motion. An example of the effective role of the ε phase is in the high-Mn Hadfield steels (14 % Mn), which in part work-harden by the formation of ε-martensite [17].

The improvements in low-temperature toughness exhibited by Fe–17Mn can be attributed to the aforementioned mechanisms – in particular, to the stress-induced phase transformations $\gamma \rightarrow \varepsilon$ and $\varepsilon \rightarrow \alpha$. According to the literature [18, 19] the transformation sequence will start with the appearance of microtwins, followed by the ε phase and then the α phase. Evidence for the stress-induced martensitic transformation was given by TEM observations of deformed sections in a specimen impacted at − 196 °C after tempering at 550 °C (Fig. 7). An examination of this microstructure indicated that the transmission of martensitic deformation occurs primarily by the $\varepsilon \rightarrow \alpha$ transformation.

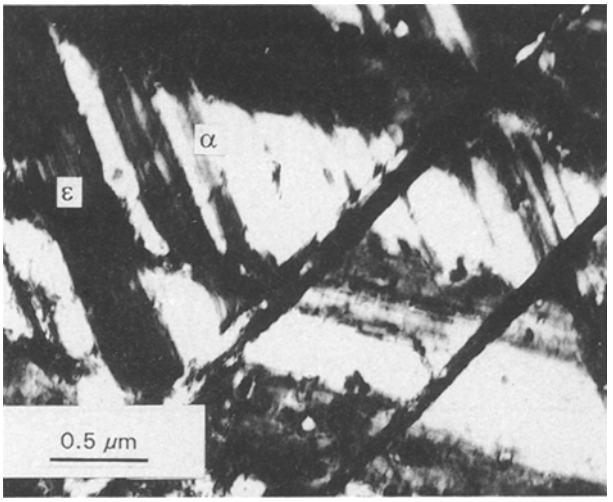

Figure 7 TEM micrograph of Fe–17Mn alloy tempered at 550 °C and impacted at − 196 °C, showing relative proportions of α- and ε-martensites.

A metallographic estimation of the area corresponding to the α phase gives a 3 to 2 ratio of α to ε, suggesting an overall increase in the α phase promoted by the alloy deformation.

Finally, alloy toughening is expected from the ε → α transformation due to its associated positive volume increase. Volume expansion is expected to contribute to the alloy fracture toughness by its effect on crack closure [20]. In particular, the hydrostatic component of the stress concentrations at the crack tip can be effectively reduced by the ε → α transformation [2]. Consequently, additional energy has to be supplied for crack propagation, resulting in improved cryogenic toughness.

5. Conclusions

1. Low-temperature embrittlement in an Fe–17Mn alloy was found to be related to temper embrittlement in the temperature range 400–450 °C.

2. There was no evidence of alloy brittleness induced by the presence of ε-martensite in this alloy.

3. The ε-martensite content consistently increased with increasing tempering temperatures and reached a maximum volume fraction at 600 °C tempering.

4. No apparent effect of the volume fraction of ε-martensite was found on the room-temperature toughness of Fe–17Mn alloy. However, at − 196 °C the alloy impact toughness exhibited appreciable improvements with increasing volume fractions of ε-martensite.

5. TEM of deformed sections of impacted specimens indicated that the major contribution to alloy toughness was through the ε → α transformation.

References

1. H. J. LEE and J. W. MORRIS, *Metall. Trans.* **14A** (1983) 913.
2. T. HORIUCHI, R. OGAWA and M. SHIMADA, *Adv. Cryog. Eng. Mater.* **32** (1986) 33.
3. J. NAMEKATA and Y. KONDO, *J. Jpn. Soc. Strength Fract. Mater.* **22** (1987) 1.
4. Y. N. PETROV, T. F. VOLYNOVA, I. A. YAKUBSTOV, I. B. MEDOV and V. M. MNASIN, *Phys. Met. Metall.* **68** (1989) 169.
5. K. M. CHANG and J. W. MORRIS Jr, *Metall. Trans.* **10A** (1979) 1377.
6. M. NIIKURA and J. W. MORRIS Jr, *ibid.* **11A** (1980) 1531.
7. N. NASIM and E. WILSON, *ibid.* **11A** (1980) 1625.
8. Y. G. KIM and C. Y. LIM, *ibid.* **19A** (1988) 1625.
9. A. SATO, K. SOMA and T. MORI, *Acta Metall.* **30** (1982) 1901.
10. K. H. HWANG, C. M. WAN and J. G. BYRNE, *Scripta Metall. Mater.* **24** (1990) 979.
11. U. R. LENEL and B. R. KNOTT, *Metall. Trans.* **18A** (1987) 847.
12. M. A. FILIPPOV, V. Y. LUGOVYKH, S. STUDENOK and M. Y. POPTSOV, *Phys. Met. Metall.* **66** (1988) 156.
13. P. LI, S. L. CHU, C. P. CHOU and F. C. CHEN, *Scripta Metall. Mater.* **25** (1991) 1869.
14. D. DUCHATEAU and M. GUTTMANN, *Acta Metall.* **29** (1981) 1291.
15. H. YOSHIMURA, T. SHIMIZU, H. YADA and K. KITAJIMA, *Trans. ISIJ* **20** (1980) 187.
16. L. LONGSHENG, *Metallography* **15** (1982) 355.
17. B. K. ZUIDEMA, D. K. SUBRAMANYAM and W. C. LESLIE, *Metall. Trans.* **18A** (1987) 1629.
18. A. H. GRAHAM and J. L. YOUNGBLOOD, *ibid.* **1** (1970) 423.
19. L. E. MURR and F. Z. GRACE, *Trans. TMS–AIME* **245** (1969) 2225.
20. G. B. OLSON and M. COHEN, *Metall. Trans.* **13A** (1982) 1907.

Received 7 October 1992
and accepted 3 February 1994